







# Fair and Efficient Spectrum Sharing in Unlicensed Bands: Does Number of Links Matter?

Yingqi Lin , Xinghua Sun , *Member, IEEE*, Yayu Gao , *Member, IEEE*, Wen Zhan , *Member, IEEE*, Xijun Wang , *Member, IEEE*, and Xiang Chen , *Member, IEEE*

**Abstract**—The rapid growth of mobile data traffic has become a great challenge to the licensed spectrum in scarcity. Driven by this, deploying networks in unlicensed bands has been drawing significant attention. This work is devoted to study the impact of the number of links on optimal coexistence performance between Licensed-Assisted Access (LAA) and WiFi in unlicensed bands. In particular, we consider three coexistence cases, including 1) single LAA link coexisting with single WiFi link; 2) single LAA link coexisting with multiple WiFi links; 3) multiple LAA links coexisting with multiple WiFi links. The throughput performance in all the three cases is characterized as explicit expressions, based on which the maximum total throughput under the throughput fairness and the corresponding optimal initial backoff window sizes are derived. A systematic comparison among the optimal performance of the three cases is conducted, and it is found that while the maximum total throughput is insensitive to the change of the number of multiple links, the drastic change from single link to multiple links in one network would lead to fierce internal competition in that network, and thus deteriorates both the optimal throughputs of the coexisting network and WiFi. This work sheds important light on the realization of fair and efficient spectrum sharing.

**Index Terms**—Spectrum-sharing, throughput optimization, coexistence fairness, listen-before-talk.

## I. INTRODUCTION

THE mobile communications have undergone an evolution of unprecedented speed in the last decade, making the

Manuscript received 14 August 2022; revised 14 January 2023; accepted 16 February 2023. Date of publication 28 February 2023; date of current version 18 July 2023. This work was supported in part by the National Key R&D Program of China under Grant 2021YFA0716600, in part by the National Natural Science Foundation of China under Grants 61972172, 62001524, and 62271513, in part by the Key Research and Development Project of Hubei Province under Grants 2020BAA02 and 2021EHB015, in part by the Guangdong Basic and Applied Basic Research Foundation under Grant 2021A1515012631, and in part by the Shenzhen Science and Technology Program under Grant RCBS20210706092408010. The review of this article was coordinated by Prof. Li Wang. (*Corresponding author: Xinghua Sun.*)

Yingqi Lin is with the School of Electronics and Communication Engineering, Shenzhen Campus of Sun Yat-sen University, Guangdong 518107, China. She is now with the ETH Zurich, Switzerland (e-mail: linyq39@mail2.sysu.edu.cn).

Xinghua Sun and Wen Zhan are with the School of Electronics and Communication Engineering, Shenzhen Campus of Sun Yat-sen University, Guangdong 518107, China (e-mail: sunxinghua@mail.sysu.edu.cn; zhanw6@mail.sysu.edu.cn).

Yayu Gao is with the School of Electronic Information and Communication, Huazhong University of Science and Technology, Wuhan 430074, China (e-mail: yayugao@hust.edu.cn).

Xijun Wang and Xiang Chen are with the School of Electronics and Information Technology, Sun Yat-sen University, Guangdong 510275, China (e-mail: wangxijun@mail.sysu.edu.cn; chenxiang@mail.sysu.edu.cn).

Digital Object Identifier 10.1109/TVT.2023.3250493

shortage of licensed spectrum resource an imperative issue. Both academia and industry have turned their attention towards efficient usage of unlicensed spectrum. Deploying networks simultaneously in licensed and unlicensed bands is then deemed as an effective approach to deal with the exponentially increasing mobile data traffic [1], [2].

The network operation in unlicensed bands inevitably affects the performance of incumbent technology in the same band, i.e., the WiFi. Hence, how to guarantee a fair and efficient coexistence becomes a critical problem [3]. In fact, numerous studies have observed that the deployment in unlicensed channel might lead to negative influence [4], [5], [6], [7], [8]. Specifically, simulations in [8] indicated that WiFi would be severely impacted by LTE transmissions as its throughput would reduce by 70% or even 100%.

In this regard, the 3rd Generation Partnership Project (3GPP) has standardized Licensed-Assisted Access (LAA) to address the challenge by forcing LTE to adopt a similar access mechanism as that of WiFi [9]. According to the definition, LAA is expected to adopt listen-before-talk (LBT) mechanism, and thus a coexisting network with LAA is required to sense the availability of channel before transmitting [10], [11]. In addition to LAA-WiFi coexistence in 5 GHz unlicensed bands, Federal Communications Commission (FCC) has opened up 1.2 GHz in 6 GHz bands for unlicensed access [12], [13]. Furthermore, 3GPP included the specification for 5G New Radio Unlicensed (NR-U) to operate in 6 GHz in its Release 16 [14]. As a successor to LAA, 5G NR-U shares a similar MAC scheme with LAA [15]. The spectrum sharing between 5G NR-U and WiFi, likewise, is also confronted with the requirement of fairness and efficiency [16], [17], [18], [19], [20]. In this paper, we concentrate on LAA in unlicensed bands. While providing a deeper understanding of the fair and efficient coexistence between LAA and WiFi, our work could also contribute to developing coexistence scheme for the upcoming 5G NR-U in unlicensed spectrum.

## A. Impact of Network Parameters

Plenty of work has analyzed the influence brought by system parameters. For example, both the initial backoff window size and the successful transmission time of unlicensed access network,  $W^{(BS)}$  and  $\tau_T^{(BS)}$ , have been shown to have crucial impacts on the performance of coexistence system [21], [22], [23], [24]. In particular, the channel access fairness was achieved in [21] by optimizing the contention window size of LTE.

According to [22], a larger successful transmission time of LTE  $\tau_T^{(BS)}$  would lead to better LTE throughput, and the LTE throughput decreases as the initial backoff window size of LTE  $W^{(BS)}$  increases [22], [23]. When the network parameters are properly adjusted to achieve a proportional fair channel time allocation, as [24] showed, a larger  $\tau_T^{(BS)}$  could improve WiFi throughput performance.

Besides  $W^{(BS)}$  and  $\tau_T^{(BS)}$ , intuitively, the number of links would greatly affect the performance of the coexistence system. In fact, 3GPP's study on LAA has presented three coexistence scenarios, including downlink-only (DL-only) LAA coexisting with DL-only WiFi, DL-only LAA coexisting with DL+uplink (UL) WiFi, and DL+UL LAA coexisting with DL+UL WiFi [9]. In this paper, both the downlink and uplink are referred to as "links".<sup>1</sup> Corresponding to 3GPP's study, the coexistence scenarios studied in this paper include 1) Case 1: single LAA link versus single WiFi link; 2) Case 2: single LAA link versus multiple WiFi links; 3) Case 3: multiple LAA links versus multiple WiFi links.

The evolution of 3GPP releases continuously enriched the definitions of coexistence scenarios, which naturally drives to study whether they would provide different levels of performance. In 3GPP Release 13, only DL transmissions of LAA are allowed to have unlicensed access. Later in Release 14, UL transmissions are also included. As for 5G NR-U, both DL and UL transmissions are employed in the unlicensed channel. This motivates to see whether the increment of the number of links could bring performance improvement.

There have been numerous discussions on the influence of the variation of links. In particular, numerical results in [22] considered only one LTE eNB with DL transmissions, where it was found that the increment of WiFi stations reduces the LTE throughput, while the WiFi throughput initially increases as the number of WiFi stations increases, and then decreases after it reaches a certain value. In [26], it was revealed that when 3GPP fairness is guaranteed in Case 2, the successful airtime of LTE and WiFi would both decrease as the number of WiFi stations increases. Analytical results for Case 3 were developed in [27]. It was shown that with the total number of LTE eNBs and WLAN APs in DL fixed at 20, a larger number of LTE eNBs leads to higher LTE throughput and worse total throughput. Moreover, it was indicated that in Case 3, more WiFi APs might result in lower WiFi throughput [28] and lower total throughput [29].

The comparison of different coexistence scenarios was further presented in a few studies. In particular, the comparison of Case 1 and Case 3 in [30] indicated that Case 1 provides better LTE throughput and WiFi throughput. Case 1 and Case 2 were compared in [22], where it was found that Case 1 has higher LTE throughput than that of Case 2. Similarly, the discussion of Case 1 and Case 2 in [31] suggested that by adopting proper

parameters, the collisions among WiFi stations could be better balanced in Case 2.

All the aforementioned studies, nevertheless, evaluated performance given system parameters. As such, comparison of scenarios might lead to inconsistent observations due to different parameter configurations. In particular, some studies found that the increment of the number of links in one network may improve its own performance [22], [27], and yet others held an opposite view [26], [28]. In fact, if the comparison is not conducted in terms of performance limit, the impact brought by the variation of the number of links would largely depend on system parameters such as the initial backoff window size. This motivates us to make a more sound comparison of all the three cases based on network optimal performance.

The characterization of the network optimal performance, unfortunately, was in lack in previous studies. To be specific, a great deal of studies evaluated LAA-WiFi coexistence performance solely from simulations [32], [33], [34], [35]. On the other hand, although some studies proposed analytical models [22], [27], [28], [30], [36], [37], [38], the performance characterization needs to solve a set of nonlinear equations. The implicit nature of the solution hinders further optimization. In our previous work [39], an analytical model has been proposed for Case 2, based on which the optimal network throughput performance was characterized. For the other two cases, nevertheless, the optimal network performance remains largely unknown. Such deficiency becomes an impediment to determining whether the inclusion of uplink transmissions is beneficial. Therefore, there is a need to characterize optimal performance of the other two cases, based on which a consistent and sound performance comparison can be made.

## B. Our Contributions

In this work, we first propose an analytical model for Case 1. By extending the model in [39], the behaviour of each head-of-line (HOL) packet in network is characterized by a discrete-time Markov renewal process, with which the performance of the coexisting network and WiFi is further analyzed. Particularly, the steady-state probabilities of successful transmissions of HOL packets of the coexisting network and WiFi are obtained, both of which are shown to be dependent on access parameters of two networks. The throughputs of the coexisting network and WiFi are further characterized as explicit expressions of system parameters. By conducting a comparison of all three scenarios, we show that the trend of network throughput when the number of links changes highly depends on the initial backoff window size.

In order to reach a fair coexistence, we consider throughput fairness that the throughput ratio between WiFi network and coexisting network maintains a target value. By jointly optimizing the initial backoff window sizes of two networks, the maximum total throughput is characterized under the throughput fairness. A systematic comparative study of the maximum total throughputs in all three cases is then conducted. It is found that: 1) In Case 2 or Case 3, as long as the scenario does not change, the variation in the number of links would not impact

<sup>1</sup>Such consideration would not affect the analysis of LAA-WiFi coexistence in this work. The reason lies in the transmission protocol and collision model we consider. According to IEEE 802.11 DCF protocol [25] and LAA mechanism indicated in 3GPP Rel. 13 [9], no matter downlink or uplink, they follow the same rule to compete for the chance to access the channel. In addition, with the classical collision model adopted in this paper, what affects network performance is the number of links, instead of the types that links belong to.

optimal throughput performance, since the competition caused by the increment of the number of links could be balanced by carefully adjusting the initial backoff window sizes. 2) Comparing three coexistence scenarios, if the number of links in one network changes drastically from single to multiple, then both the throughputs of the coexisting and WiFi networks would degrade. This is because that with the constraint of throughput fairness, a constant level of inter-competition between two networks can be guaranteed. Nevertheless, the abrupt increment of links from single to multiple yields intra-competition in that network, resulting in the throughput degradation of its own as well as the other network. 3) Although Case 1 is seldom the focus of previous studies, our work shows that Case 1 can achieve the best optimal throughput performance among all the three cases.

The major contributions of this paper are summarized as:

- We establish an analytical model for the coexistence scenario of single LAA link and single WiFi AP, based on which the throughput performance is characterized as explicit expressions of system parameters. The maximum total throughputs under the throughput fairness of Case 1 and Case 3 are further obtained by optimizing over the initial backoff window sizes of the coexisting and WiFi networks.
- Based on the optimal total throughput under the throughput fairness, the comparison among the three cases indicates that the variation of the number of links in one case can be balanced by jointly tuning initial backoff window sizes. However, the drastic change of links from single to multiple would deteriorate both networks' performance. As a result, Case 1 outperforms the other two cases, which suggests that the inclusion of UL transmissions might lead to performance deterioration.

The rest of this paper is structured as follows: system model and preliminary analysis of the coexistence are described in Section II. Section III characterizes the throughput performance of the coexistence system and the maximum total throughput of coexisting network and WiFi under the throughput fairness. In Section IV, a comparison among the throughput performances of three coexistence scenarios is drawn, and is verified by simulation results. Section V concludes the whole research.

## II. SYSTEM MODEL AND PRELIMINARY ANALYSIS

Consider the scenario given in Fig. 1, where a cellular base station (BS) coexists with a WiFi network. With the objective of dealing with increasing mobile data traffic and shortage of licensed channel, the BS shares a common unlicensed band with the WiFi AP. In our previous study [39], Case 2, i.e., single BS coexists with multiple WiFi links, was considered. In this paper, we adopt the same system model as that in [39], except that here we consider Case 1, i.e., single BS coexists with single WiFi AP. Saturated conditions are assumed, i.e., the links in coexistence system continuously have packets to send. The classic collision model is adopted such that one packet transmission can only be successful when there are no simultaneous transmissions. Both the coexisting and WiFi networks adopt the request-to-send/clear-to-send (RTS/CTS) mechanism to mitigate the hidden terminal problem.

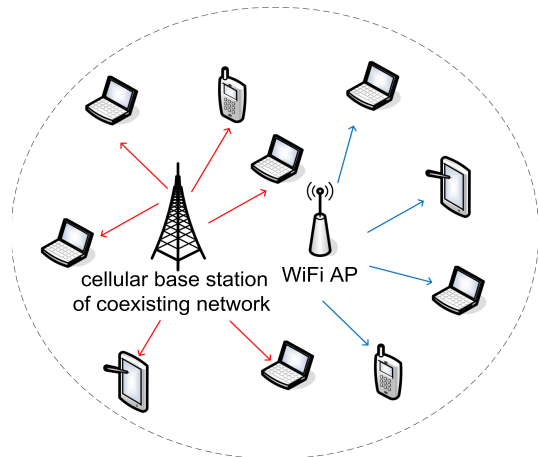


Fig. 1. Scenario of the coexistence with a WiFi network.

For the WiFi network, the WiFi AP makes transmissions conforming to IEEE 802.11 DCF protocol [25]. Let  $W^{(W)}$  denote the initial backoff window size of WiFi. When WiFi AP has a fresh HOL packet, it chooses a value from  $\{0, \dots, W^{(W)}\}$  at random, and this value diminishes by one at each idle time slot. If the counter reaches zero and the channel is idle, then the WiFi AP will make a transmission request. After the  $i$ th transmission failure, the window size becomes  $W_i^{(W)}$ . Without loss of generality, in this paper it is assumed that

$$W_i^{(W)} = W^{(W)} \cdot \omega(i), \quad (1)$$

and that the WiFi network adopts binary exponential backoff. In particular,  $\omega(i) = \min\{2^i, 2^{K^{(W)}}\}$ ,  $i = 0, 1, \dots$ , in which  $K^{(W)}$  represents the cutoff phase.

For the coexisting network, when it employs the Category 3 LBT mechanism, the BS picks a value from  $\{0, \dots, W^{(BS)}\}$  at random if it has a packet ready to transmit, where  $W^{(BS)}$  represents the contention window size. Contrary to a fixed window size in Category 3, for BS adopting Category 4 LBT mechanism, as the definition in 3GPP Rel. 13 indicates [9], its contention window is of variable size. The contention window size of the coexisting network will become  $W_i^{(BS)}$  after the  $i$ th transmission failure. Assume that

$$W_i^{(BS)} = W^{(BS)} \cdot \zeta(i), \quad (2)$$

in which  $\zeta(i) = \min\{2^i, 2^{K^{(BS)}}\}$ ,  $i = 0, 1, \dots$  for coexisting network with the Category 4 LBT mechanism, and  $K^{(BS)}$  represents the cutoff phase. The Category 3 LBT mechanism can then be regarded as a special circumstance of Category 4 with  $K^{(BS)} = 0$ .

### A. State Characterization of HOL Packets

In this section, we will extend the analytical framework put forward in [39] to Case 1, i.e., one BS versus one WiFi link. Note that the characterization of Case 1 cannot be obtained by substituting the number of WiFi links equaling one into the corresponding expressions in [39], where a large number of WiFi links was assumed. In particular, a discrete-time Markov renewal process is established to model the behavior of each HOL packet,



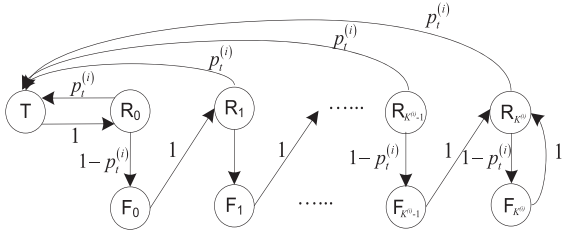


Fig. 2. Embedded Markov chain  $\{X_j^{(i)}\}$  of the state transition process of a single HOL packet, in which  $i \in \{BS, W\}$  denote the coexisting network and WiFi, respectively.

as shown in Fig. 2, where the states of HOL packet can be categorized into: waiting to request (State  $R_t$ ,  $t = 0, \dots, K^{(i)}$ ), collision (State  $F_t$ ,  $t = 0, \dots, K^{(i)}$ ), and successful transmission (State T).

By following a similar derivation as that in [39], the limiting state probabilities of the Markov renewal process  $(\mathbf{X}^{(i)}, \mathbf{V}^{(i)})$  are given by

$$\tilde{\pi}_j^{(i)} = \frac{\pi_j^{(i)} \cdot \tau_j^{(i)}}{\sum_{l \in S^{(i)}} \pi_l^{(i)} \cdot \tau_l^{(i)}}, \quad (3)$$

$i \in \{BS, W\}$ , where  $\{\pi_j^{(i)}\}_{j \in S^{(i)}}$  denotes the steady-state probability distribution of the embedded Markov chain,  $S^{(i)}$  is the state space of  $\mathbf{X}^{(i)}$  and  $\tau_j^{(i)}$  represents the mean holding time in each state,  $j \in S^{(i)}$ . The probabilities of being in State T of the HOL packet,  $\tilde{\pi}_T^{(i)}$ ,  $i \in \{BS, W\}$ , can then be given by

$$\tilde{\pi}_T^{(i)} = \frac{1}{1 + \frac{\tau_F^{(i)}}{\tau_T^{(i)}} \cdot \frac{1-p^{(i)}}{p^{(i)}} + \frac{1}{\alpha \tau_T^{(i)}} \sum_{j=0}^{\infty} (1-p^{(i)})^j \cdot \frac{1+W_j^{(i)}}{2}}, \quad (4)$$

where  $p^{(i)}$ ,  $i \in \{BS, W\}$  denote the steady-state probabilities of successful transmissions of HOL packets given that the channel is idle, and the steady-state probability of sensing the channel idle,  $\alpha$ , is given by

$$\alpha = 1/(1 + \tau_F + (\tau_T^{(BS)} - \tau_F)p^{(BS)} + (\tau_T^{(W)} - \tau_F)p^{(W)} + (\tau_F - \tau_T^{(BS)} - \tau_T^{(W)})p^{(BS)}p^{(W)}), \quad (5)$$

which is obtained by following a similar derivation as that in [41], and is different from  $\alpha$  in Case 2 [39] since the competition level in coexistence system changes as the number of links changes.

### B. Probability of Successful Transmission

In this work, network throughput is rendered as the metric for efficiency, which is defined as average number of HOL packets that are successfully transmitted per unit time. In order to characterize network throughput, the steady-state probabilities of successful transmissions of HOL packets given that the channel idle of the coexisting network and WiFi,  $p^{(BS)}$  and  $p^{(W)}$ , should first be determined. In the following, we will illustrate the derivation of  $p^{(BS)}$  and  $p^{(W)}$ .

Consider the BS in coexisting network. If the WiFi AP does not compete to access the channel, BS transmission will be successful. As a result, the probability of successful transmission

of HOL packet given that the channel is idle in the coexisting network,  $p^{(BS)}$ , is given by

$$p^{(BS)} = \Pr \{ \text{the WiFi AP does not attempt to access the channel} | \text{channel is idle} \}. \quad (6)$$

As the Markov chain in Fig. 2 illustrates, the steady-state probability that WiFi AP attempts to access the channel given that the channel is idle can be given by  $\sum_{i=0}^{K^{(W)}} \tilde{\pi}_{R_i}^{(W)} r_i^{(W)}$ . According to [41], given that the channel is idle,  $r_i^{(W)} = \frac{2}{1+W_i^{(W)}}$  denotes the conditional probability of the transmission request of a State- $R_i$  HOL packet in the WiFi network given that the channel is idle. It can therefore be obtained that

$$p^{(BS)} = 1 - \sum_{i=0}^{K^{(W)}} \tilde{\pi}_{R_i}^{(W)} r_i^{(W)} = 1 - \frac{1}{\alpha p^{(W)}} \cdot \frac{\tilde{\pi}_T^{(W)}}{\tau_T^{(W)}}, \quad (7)$$

according to (3). By substituting (4) into (7), it can be obtained that

$$p^{(BS)} = 1 - \frac{2}{1 + \sum_{i=0}^{\infty} p^{(W)} (1-p^{(W)})^i W_i^{(W)}}. \quad (8)$$

For the WiFi AP, likewise, its transmission is successful when the BS does not try to access the channel. As a result, the probability of successful transmission of HOL packet given that the channel is idle in the WiFi network,  $p^{(W)}$ , is given by

$$p^{(W)} = \Pr \{ \text{the BS does not attempt to access the channel} | \text{channel is idle} \}. \quad (9)$$

Similarly, we have

$$p^{(W)} = 1 - \sum_{i=0}^{K^{(BS)}} \tilde{\pi}_{R_i}^{(BS)} r_i^{(BS)} = 1 - \frac{1}{\alpha p^{(BS)}} \cdot \frac{\tilde{\pi}_T^{(BS)}}{\tau_T^{(BS)}}. \quad (10)$$

Substituting (4) into (10) results in

$$p^{(W)} = 1 - \frac{2}{1 + \sum_{i=0}^{\infty} p^{(BS)} (1-p^{(BS)})^i W_i^{(BS)}}. \quad (11)$$

We can observe that  $p^{(BS)}$  and  $p^{(W)}$  obtained above for Case 1 are different from that in Case 2 [39] since the degree of competition has changed, and they cannot be derived from [39] by simply letting the number of WiFi links equal to 1. A separate analysis is then needed here for the characterization of the coexistence performance in Case 1.

By jointly solving (8) and (11), we can obtain the steady-state points of the coexisting network and WiFi, which are shown to be related to the sequences of backoff window sizes  $\{W_i^{(BS)}\}_{i=0,1,\dots}$  and  $\{W_i^{(W)}\}_{i=0,1,\dots}$ . For instance, if a fixed backoff window size is adopted in coexisting network and an exponential backoff is employed in WiFi, i.e.,  $\omega(i) = q^{-i}$ ,  $q \in (0, 1)$ ,  $i = 0, 1, \dots$ , then it can be derived that

$$p^{(BS)} = \mathbb{W}_0 \left( \frac{W^{(BS)} + 1}{W^{(BS)} - 1} \cdot \frac{2(1-q)}{W^{(W)}q} \cdot \exp \left( \frac{2}{W^{(W)}q} \right) \right) - \frac{2}{W^{(W)}q} + 1, \quad (12)$$

and

$$p^{(W)} = \frac{W^{(BS)} - 1}{W^{(BS)} + 1}. \quad (13)$$

### III. THROUGHPUT CHARACTERIZATION AND OPTIMIZATION

We have introduced three coexistence scenarios above, including 1) Case 1: single BS versus single WiFi link; 2) Case 2: single BS versus multiple WiFi links; 3) Case 3: multiple BSs versus multiple WiFi links. In this section, the throughputs of the coexistence system under all three cases will be characterized. Furthermore, the maximum total throughput of coexisting network and WiFi under throughput fairness as well as the corresponding initial backoff window sizes in optimal situation will also be determined.

#### A. Throughput Characterization

Let us first consider Case 1 that one BS coexists with one WiFi link. In saturated condition, each link's throughput equals the service rate of its queue,  $\tilde{\pi}_T^{(i)}$ . Based on this, the throughput of the WiFi network is equivalent to the throughput of WiFi AP in downlink as only the downlink transmissions from AP are considered in Case 1, and the WiFi throughput can therefore be written as  $\hat{\lambda}_{\text{out}}^{1,(W)} = \tilde{\pi}_T^{(W)}$ . According to (5) and (7), we then have

$$\begin{aligned} \hat{\lambda}_{\text{out}}^{1,(W)} &= \tau_T^{(W)} p^{(W)} (1-p^{(BS)}) / \left( 1 + \tau_F + (\tau_T^{(BS)} - \tau_F) p^{(BS)} \right. \\ &\quad \left. + (\tau_T^{(W)} - \tau_F) p^{(W)} + (\tau_F - \tau_T^{(BS)} - \tau_T^{(W)}) p^{(BS)} p^{(W)} \right). \end{aligned} \quad (14)$$

For the coexisting network, likewise, only the downlink transmissions of the BS via unlicensed channel are considered, so the throughput of the coexisting network is given by  $\hat{\lambda}_{\text{out}}^{1,(BS)} = \tilde{\pi}_T^{(BS)}$ . We then have

$$\begin{aligned} \hat{\lambda}_{\text{out}}^{1,(BS)} &= \tau_T^{(BS)} p^{(BS)} (1-p^{(W)}) / \left( 1 + \tau_F + (\tau_T^{(BS)} - \tau_F) p^{(BS)} \right. \\ &\quad \left. + (\tau_T^{(W)} - \tau_F) p^{(W)} + (\tau_F - \tau_T^{(BS)} - \tau_T^{(W)}) p^{(BS)} p^{(W)} \right), \end{aligned} \quad (15)$$

according to (5) and (10).

For Case 2 that one BS coexists with multiple WiFi links, the throughput of the WiFi network under this circumstance has been obtained in [39] as

$$\begin{aligned} \hat{\lambda}_{\text{out}}^{2,(W)} &= -\tau_T^{(W)} p^{(W)} \ln p^{(BS)} / \left( 1 + \tau_F + (\tau_T^{(BS)} - \tau_F) p^{(BS)} \right. \\ &\quad \left. - \tau_T^{(BS)} p^{(W)} - (\tau_T^{(W)} - \tau_F) p^{(W)} \ln p^{(BS)} \right), \end{aligned} \quad (16)$$

and the throughput of the coexisting network is identical to the downlink throughput of BS, which can be written as

$$\begin{aligned} \hat{\lambda}_{\text{out}}^{2,(BS)} &= \tau_T^{(BS)} (p^{(BS)} - p^{(W)}) / \left( 1 + \tau_F + (\tau_T^{(BS)} - \tau_F) p^{(BS)} \right. \\ &\quad \left. - \tau_T^{(BS)} p^{(W)} - (\tau_T^{(W)} - \tau_F) p^{(W)} \ln p^{(BS)} \right). \end{aligned} \quad (17)$$

In Case 3, both the downlink and uplink transmissions of the coexisting and WiFi networks are considered. Therefore, in WiFi

network, the WiFi AP as well as the other links have competition for unlicensed band in order to support their downlink or uplink transmissions. We take  $n^{(W)}$  to represent the total number of links in the WiFi network. In the coexisting network, on the other hand, multiple BSs also compete to transmit, and we denote the total number of links as  $n^{(BS)}$ . According to [42], we have the following expressions that indicate throughputs of the coexisting network and WiFi under such circumstance. The network throughput  $\hat{\lambda}_{\text{out}}^{3,(g)}$  of the coexisting network  $g = BS$ , and of the WiFi network  $g = W$ , are given by

$$\hat{\lambda}_{\text{out}}^{3,(g)} = \frac{2\alpha_A n^{(g)} p_A \tau_T^{(g)}}{\sum_{i=0}^{\infty} p_A (1-p_A)^i \cdot W_i^{(g)} + (1-p_A)^{K^{(g)}} \cdot W_{K^{(g)}}^{(g)}}, \quad (18)$$

$g \in \{BS, W\}$ , where  $p_A$  denotes the steady-state point, i.e., the probability of successful transmissions of HOL packets given that the channel is idle of BSs and WiFi links, which is given by

$$\begin{aligned} p &= \exp \left\{ -\frac{1}{\alpha_A p} \sum_{g=BS,W} \frac{\hat{\lambda}_{\text{out}}^{3,(g)}}{\tau_T^{(g)}} \right\} \\ &= \exp \left\{ -\sum_{g=BS,W} \frac{2n^{(g)}}{\sum_{i=0}^{\infty} p(1-p)^i \cdot W_i^{(g)} + (1-p)^{K^{(g)}} \cdot W_{K^{(g)}}^{(g)}} \right\}, \end{aligned} \quad (19)$$

and the probability that the channel is idle,  $\alpha_A$ , can be written as

$$\alpha_A = \frac{1}{1 + \tau_F - \tau_F p_A - \left( \frac{\sum_{g=BS,W} \tau_T^{(g)} X^{(g)}}{\sum_{g=BS,W} X^{(g)}} - \tau_F \right) p_A \ln p_A}, \quad (20)$$

where  $X^{(g)} = \frac{n^{(g)} p_A}{\sum_{i=0}^{\infty} p_A (1-p_A)^i \cdot W_i^{(g)} + (1-p_A)^{K^{(g)}} \cdot W_{K^{(g)}}^{(g)}}$ .

It is indicated in (14), (15), (16), (17) and (18) that both the throughputs of the coexisting and WiFi networks,  $\hat{\lambda}_{\text{out}}^{(BS)}$  and  $\hat{\lambda}_{\text{out}}^{(W)}$ , are strongly related to the conditional probabilities of successful transmissions of HOL packets when the channel is idle,  $p^{(BS)}$  and  $p^{(W)}$ . Thus the throughputs further rely on the sequences of backoff window sizes  $\{W_i^{(BS)}\}_{i=0,1,\dots}$  and  $\{W_i^{(W)}\}_{i=0,1,\dots}$ . In other words, the initial backoff window sizes play a crucial role when considering the coexistence performance. In the following, by jointly adjusting the initial backoff window sizes, we will optimize the coexistence system in unlicensed spectrum to reach high efficiency while guaranteeing fairness.

#### B. Fairness-Constrained Throughput Optimization

To maintain a fair and efficient coexistence is one of the most crucial issues relating to the spectrum sharing in unlicensed bands. A variety of notions for fairness have been put forward to satisfy the requirements in diverse systems. Here, we adopt the throughput fairness proposal in our previous work [39], [40]. Specifically, we use  $\gamma$  to represent the target throughput ratio

between the WiFi and the coexisting network, i.e.,  $\frac{\hat{\lambda}_{\text{out}}^{(W)}}{\hat{\lambda}_{\text{out}}^{(BS)}} = \gamma$ , where the value of  $\gamma$  is selected according to practical service needs. Let  $\hat{\lambda}_{\text{max}}^\gamma$  denote the maximum total throughput of the coexisting network and WiFi under fairness constraint. To guarantee a fair and efficient coexistence, we have the following optimization problem

$$\begin{aligned} \hat{\lambda}_{\text{max}}^\gamma &= \max_{\{W^{(BS)}, W^{(W)}\}} (\hat{\lambda}_{\text{out}}^{(W)} + \hat{\lambda}_{\text{out}}^{(BS)}) \\ \text{s.t.} \quad &\frac{\hat{\lambda}_{\text{out}}^{(W)}}{\hat{\lambda}_{\text{out}}^{(BS)}} = \gamma. \end{aligned} \quad (21)$$

For Case 1, the optimal total throughput with fairness constraint is presented in the following theorem. Moreover, the corresponding initial backoff window sizes of the BS and the WiFi AP are presented as well.

*Theorem 1:* In Case 1, the maximum total throughput of the coexisting network and WiFi under the throughput fairness can be written as

$$\hat{\lambda}_{\text{max}}^{1,\gamma} = \frac{1+\gamma}{\gamma} \cdot \frac{\tau_T^{(W)}}{\frac{\tau_T^{(W)} + \tau_F \tau_T^{(W)} (1-p^{\gamma,(BS)})}{\gamma \tau_T^{(BS)} p^{\gamma,(BS)}} + \frac{1}{1-p^{\gamma,(BS)}} + \frac{1+\gamma}{\gamma} \cdot \tau_T^{(W)}}, \quad (22)$$

where  $p^{\gamma,(BS)}$  is the single root of

$$\begin{aligned} & - \left[ \tau_T^{(W)} \tau_F p^{(BS)} + \tau_T^{(W)} + \tau_T^{(W)} \tau_F (1-p^{(BS)}) \right] \\ & \cdot (1-p^{(BS)})^2 + \gamma \tau_T^{(BS)} (p^{(BS)})^2 = 0, \end{aligned} \quad (23)$$

and  $p^{\gamma,(W)}$  is given by

$$p^{\gamma,(W)} = \frac{\gamma \tau_T^{(BS)} p^{\gamma,(BS)}}{\tau_T^{(W)} (1-p^{\gamma,(BS)}) + \gamma \tau_T^{(BS)} p^{\gamma,(BS)}}. \quad (24)$$

$\hat{\lambda}_{\text{max}}^{1,\gamma}$  can be reached when the initial backoff window sizes of BS and WiFi AP are tuned to be

$$W^{(BS)} = W^{\gamma,(BS)} = \frac{\frac{2}{-\ln p^{\gamma,(W)}} - 1}{\sum_{i=0}^{\infty} p^{\gamma,(BS)} (1-p^{\gamma,(BS)})^i \zeta(i)}, \quad (25)$$

and

$$W^{(W)} = W^{\gamma,(W)} = \frac{\frac{2}{-\ln p^{\gamma,(BS)}} - 1}{\sum_{i=0}^{\infty} p^{\gamma,(W)} (1-p^{\gamma,(W)})^i \omega(i)}, \quad (26)$$

respectively.

*Proof:* See Appendix A.  $\blacksquare$

For Case 2, the optimal total throughput under the throughput fairness has been derived in [39] as

$$\begin{aligned} \hat{\lambda}_{\text{max}}^{2,\gamma} &= \\ & \frac{1+\gamma}{\gamma} \cdot \frac{\tau_T^{(W)}}{\frac{1+\tau_F + (\tau_T^{(BS)} - \tau_F) p^{\gamma,(BS)} - \tau_T^{(BS)} p^{\gamma,(W)}}{-p^{\gamma,(W)} \ln p^{\gamma,(BS)}} + \tau_T^{(W)} - \tau_F}, \end{aligned} \quad (27)$$

where  $p^{\gamma,(BS)}$  is the single root of

$$\begin{aligned} & - \gamma \tau_T^{(BS)} \tau_F p^{(BS)} + \gamma \tau_T^{(BS)} (1 + \tau_F) (1 + \ln p^{(BS)}) \\ & - \tau_T^{(W)} (1 + \tau_F) (\ln p^{(BS)})^2 = 0, \end{aligned} \quad (28)$$

and  $p^{\gamma,(W)}$  is given by

$$p^{\gamma,(W)} = \frac{\gamma \tau_T^{(BS)} p^{\gamma,(BS)}}{\gamma \tau_T^{(BS)} - \tau_T^{(W)} \ln p^{\gamma,(BS)}}. \quad (29)$$

$\hat{\lambda}_{\text{max}}^{2,\gamma}$  can be reached if the initial backoff window sizes of BS and each WiFi link are tuned to be

$$W^{(BS)} = W^{\gamma,(BS)} = \frac{\frac{2\gamma \tau_T^{(BS)}}{-\tau_T^{(W)} \ln p^{\gamma,(BS)}} + 1}{\sum_{i=0}^{\infty} p^{\gamma,(BS)} (1-p^{\gamma,(BS)})^i \zeta(i)}, \quad (30)$$

and

$$W^{(W)} = W^{\gamma,(W)} = \frac{\frac{2n^{(W)}}{-\ln p^{\gamma,(BS)}} - 1}{\sum_{i=0}^{\infty} p^{\gamma,(W)} (1-p^{\gamma,(W)})^i \omega(i)}, \quad (31)$$

respectively.

For Case 3, the network throughput performance has been derived as (18). Based on this result, the optimal total throughput under the throughput fairness and the corresponding initial backoff window sizes can be derived as the following theorem.

*Theorem 2:* In Case 3, the maximum total throughput of the coexisting network and WiFi under the throughput fairness can be written as

$$\hat{\lambda}_{\text{max}}^{3,\gamma} = \frac{1+\gamma}{1+\gamma + \frac{\gamma \tau_T^{(BS)} + \tau_T^{(W)}}{\tau_T^{(BS)} \tau_T^{(W)}} \cdot \left( \frac{1+\tau_F - \tau_F p_A^*}{-p_A^* \ln p_A^*} - \tau_F \right)}. \quad (32)$$

The total throughput is optimized when the initial backoff window size of each BS is adjusted to be

$$\begin{aligned} W^{(BS)} &= W^{\gamma,(BS)} \\ &= \frac{2n^{(BS)} \left( 1 + \frac{\gamma \tau_T^{(BS)}}{\tau_T^{(W)}} \right)}{-\ln p_A^* \cdot \left( \sum_{i=0}^{\infty} p_A^* (1-p_A^*)^i \zeta(i) + (2-2p_A^*)^{K^{(BS)}} \right)}, \end{aligned} \quad (33)$$

and the initial backoff window size of each WiFi link is tuned to be

$$\begin{aligned} W^{(W)} &= W^{\gamma,(W)} \\ &= \frac{2n^{(W)} \left( 1 + \frac{\tau_T^{(W)}}{\gamma \tau_T^{(BS)}} \right)}{-\ln p_A^* \cdot \left( \sum_{i=0}^{\infty} p_A^* (1-p_A^*)^i \omega(i) + (2-2p_A^*)^{K^{(W)}} \right)}, \end{aligned} \quad (34)$$

where  $p_A^* = -(1 + 1/\tau_F) \mathbb{W}_0(-\frac{1}{e(1+1/\tau_F)})$ .

*Proof:* See Appendix B.

With the optimal network performance, we compare our results with other studies. In particular, Fig. 3 illustrates the total throughput of the coexisting network and WiFi, where we denote the optimal total throughput from our work as  $\hat{\lambda}_{\text{max}}^\gamma$  and the throughput evaluation as  $\hat{\lambda}_{\text{out}}$  [23], [30].  $\hat{\lambda}_{\text{max}}^\gamma$  is obtained following the optimization method proposed in Theorem 2. In

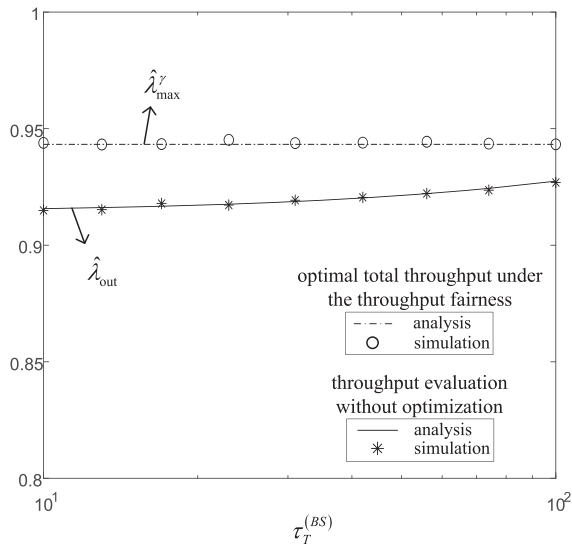


Fig. 3. Total throughput of the coexisting and WiFi networks versus the successful transmission time of the coexisting network  $\tau_T^{(BS)}$  (in unit of time slots). The number of BSs  $n^{(BS)} = 10$  and the number of WiFi links  $n^{(W)} = 50$ .  $\tau_T^{(W)} = 100$  and  $\tau_F = 10$ . For the evaluation approach from other work,  $W_i^{(W)} = W^{(W)} \cdot \omega(i)$  where  $W^{(W)} = 32$ ,  $\omega(i) = \min\{2^i, 2^{K^{(W)}}\}$  and  $K^{(W)} = 6$ .  $W_i^{(BS)} = W^{(BS)} \cdot \zeta(i)$  in which  $\zeta(i) = \min\{2^i, 2^{K^{(BS)}}\}$  and  $K^{(BS)} = 6$ .

Fig. 3, we first evaluate throughput performance according to the characterization in [23], [30]. Then we calculate the throughput ratio of WiFi and coexisting network, i.e.,  $\gamma = \frac{\hat{\lambda}_{out}^{(W)}}{\hat{\lambda}_{out}^{(BS)}}$ . For each value of throughput ratio, the corresponding optimal total throughput under the throughput fairness  $\hat{\lambda}_{max}^{\gamma}$  is derived, with system configuration remaining the same. As we can observe from Fig. 3, for any throughput ratio,  $\hat{\lambda}_{max}^{\gamma}$  is always higher than  $\hat{\lambda}_{out}$ . Our optimization method shows an improvement on network performance, contributing to the design of a fair and efficient coexistence between LAA and WiFi.

#### IV. THROUGHPUT COMPARISON AND SIMULATION RESULTS

In Section III, we have analyzed the throughputs of the coexisting network and WiFi, based on which the optimal total throughputs under the throughput fairness in three coexistence cases are further characterized. Next, we will draw a comparison among the performances of the coexistence system in all three scenarios.

##### A. Throughput Comparison Given System Parameters

With the analysis results in Section III, we now have explicit expressions of the throughputs of the coexisting network and WiFi in three coexistence cases, as (14), (15), (16), (17), and (18) show. Fig. 4(a) and (b) present comparisons among the throughput performances in three scenarios. Note that throughout this section, simulation results will also be provided to verify the analysis.

As Fig. 4(a) illustrates, when the number of links in one network increases, how its throughput performance would change

depends on the initial backoff window size. For instance, with the number of WiFi links  $n^{(W)} = 5$ , when  $W^{(BS)}$  is small, a larger  $n^{(BS)}$  reduces the throughput of coexisting network,  $\hat{\lambda}_{out}^{(BS)}$ . This is because that at this time, the internal competition emerged in coexisting network exceeds the gain from external competition with WiFi. When  $W^{(BS)}$  is large, in contrast, the increase of  $n^{(BS)}$  enhances the competitiveness of the coexisting network, leading to a higher  $\hat{\lambda}_{out}^{(BS)}$ . Recall that previous studies presented contradictory results in terms of how the number of links would affect the coexistence performance. In particular, it was indicated in [22], [27] that the increment of the number of links in one network might improve its own throughput performance, while others held an opposite view [28], [30]. Here we can see that those inconsistent observations in previous studies might come from different settings of network parameters.

Fig. 4(b) further illustrates how the total throughput,  $\hat{\lambda}_{out}$ , would change with  $W^{(BS)}$  under three coexistence scenarios. It is shown in Fig. 4(b) that with the number of BSs  $n^{(BS)} = 1$ , a larger number of WiFi links  $n^{(W)}$  leads to lower total throughput with a small  $W^{(BS)}$ . When  $W^{(BS)}$  is enlarged, however, a larger  $n^{(W)}$  results in better throughput performance. The reason is that, with a large initial backoff window, the coexisting network is less likely to access the channel. Therefore, a larger number of WiFi links  $n^{(W)}$  results in more attempts to access the channel, thus providing a higher total throughput. When  $W^{(BS)}$  is small, on the contrary, the WiFi network would face fierce competition from the coexisting network. At this time, more WiFi links would cause more intense competition, and thus the total throughput decreases. In previous studies, it was shown that a larger total number of links in the coexistence system could deteriorate the total throughput [30], and more WiFi links might also reduce the total throughput [23]. Here we can see that how the change in the number of links would affect the total throughput also depends on the initial backoff window size.

As for the impact of the successful transmission time of the coexisting network,  $\tau_T^{(BS)}$ , it is found in Fig. 5(a) that, different from observations in Fig. 4(a) and (b) that the initial backoff window size would affect the relative relationship between throughputs in three scenarios, the relationship always holds without regard to the variation of  $\tau_T^{(BS)}$ . A larger  $\tau_T^{(BS)}$ , nevertheless, would lead to a worse WiFi throughput performance and a better throughput performance of the coexisting network, since with a larger  $\tau_T^{(BS)}$ , the coexisting network would occupy the channel for a longer period of time once the network can successfully access the channel. Simulation results agree well with the analysis.

##### B. Throughput Comparison With Optimized System Parameters

In Section III, we have discussed the maximum total throughputs of the coexisting network and WiFi under the constraint of throughput fairness for three coexistence cases, as (22), (27), and (32) illustrate. In the following, we will present a comparison among the optimal total throughputs in three cases.



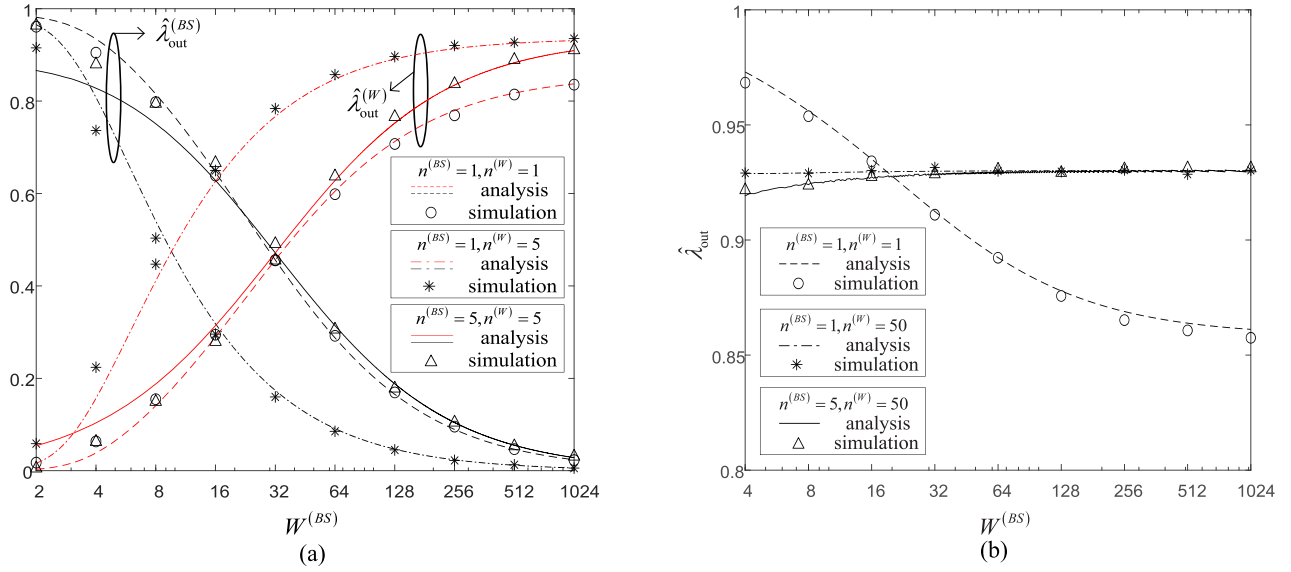


Fig. 4. (a) The throughputs of the coexisting network and WiFi,  $\hat{\lambda}_{out}^{(BS)}$  and  $\hat{\lambda}_{out}^{(W)}$ , and (b) the total throughput of the coexisting and WiFi networks versus the initial backoff window size of the coexisting network  $W^{(BS)}$  under three coexistence scenarios.  $n^{(BS)}$  and  $n^{(W)}$  denote the number of links in the coexisting network and WiFi, respectively.  $\tau_T^{(W)} = \tau_T^{(BS)} = 100$  and  $\tau_F = 10$ .  $W_i^{(W)} = W^{(W)} \cdot \omega(i)$  where  $W^{(W)} = 32$ ,  $\omega(i) = \min\{2^i, 2^{K^{(W)}}\}$  and  $K^{(W)} = 6$ .  $W_i^{(BS)} = W^{(BS)} \cdot \zeta(i)$  in which  $\zeta(i) = \min\{2^i, 2^{K^{(BS)}}\}$  and  $K^{(BS)} = 6$ .

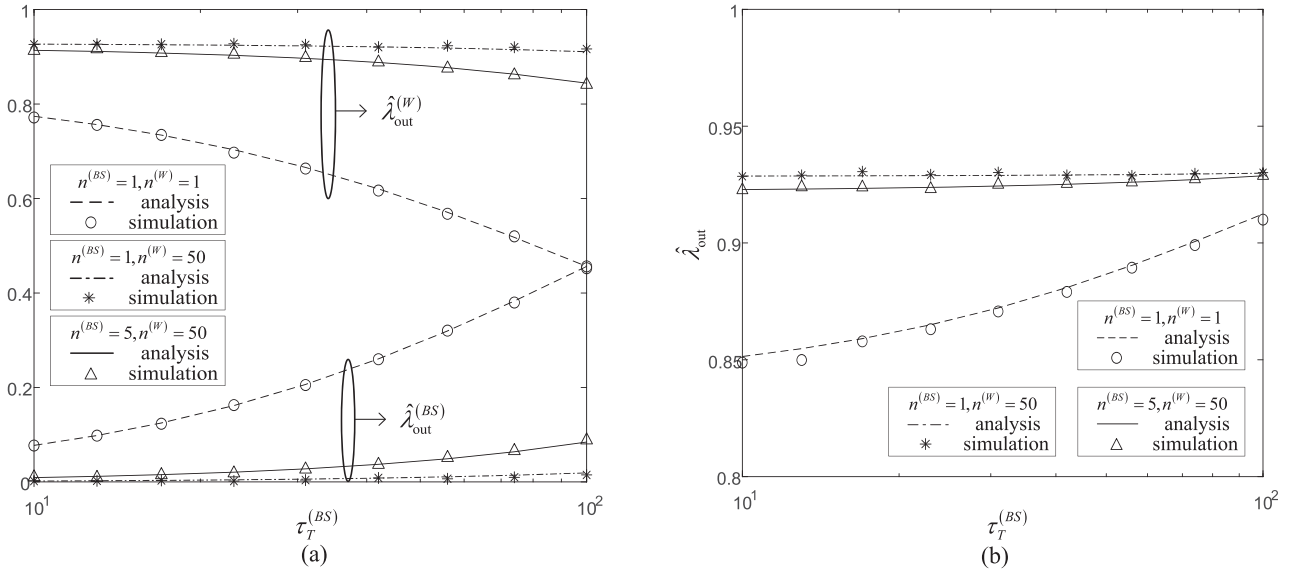


Fig. 5. (a) The throughputs of the coexisting network and WiFi,  $\hat{\lambda}_{out}^{(BS)}$  and  $\hat{\lambda}_{out}^{(W)}$ , and (b) the total throughput of the coexisting and WiFi networks versus the successful transmission time of the coexisting network  $\tau_T^{(BS)}$  (in unit of time slots) under three coexistence scenarios: 1)  $n^{(BS)} = 1, n^{(W)} = 1$ ; 2)  $n^{(BS)} = 1, n^{(W)} = 50$ ; 3)  $n^{(BS)} = 5, n^{(W)} = 50$ .  $\tau_T^{(W)} = 100$  and  $\tau_F = 10$ .  $W_i^{(W)} = W^{(W)} \cdot \omega(i)$  where  $W^{(W)} = 32$ ,  $\omega(i) = \min\{2^i, 2^{K^{(W)}}\}$  and  $K^{(W)} = 6$ .  $W_i^{(BS)} = W^{(BS)} \cdot \zeta(i)$  where  $W^{(BS)} = 32$ ,  $\zeta(i) = \min\{2^i, 2^{K^{(BS)}}\}$  and  $K^{(BS)} = 6$ .

Fig. 6(a) and (b) illustrate how the maximum total throughputs in three coexistence scenarios,  $\hat{\lambda}_{out}^{\gamma}$ , vary with the target throughput ratio between WiFi and coexisting network,  $\gamma$ , and with the successful transmission time of the coexisting network,  $\tau_T^{(BS)}$ , respectively. We can clearly observe from both Fig. 6(a) and (b) that when the total throughput is maximized under

the throughput fairness, the increment of links in one network from single to multiple not only reduces the throughput of the other network, but also leads to the decrease of this network's own throughput. Specifically, when the number of BSs in the coexisting network is fixed, the change in the number of WiFi links  $n^{(W)}$  from single to multiple results in the decrease of



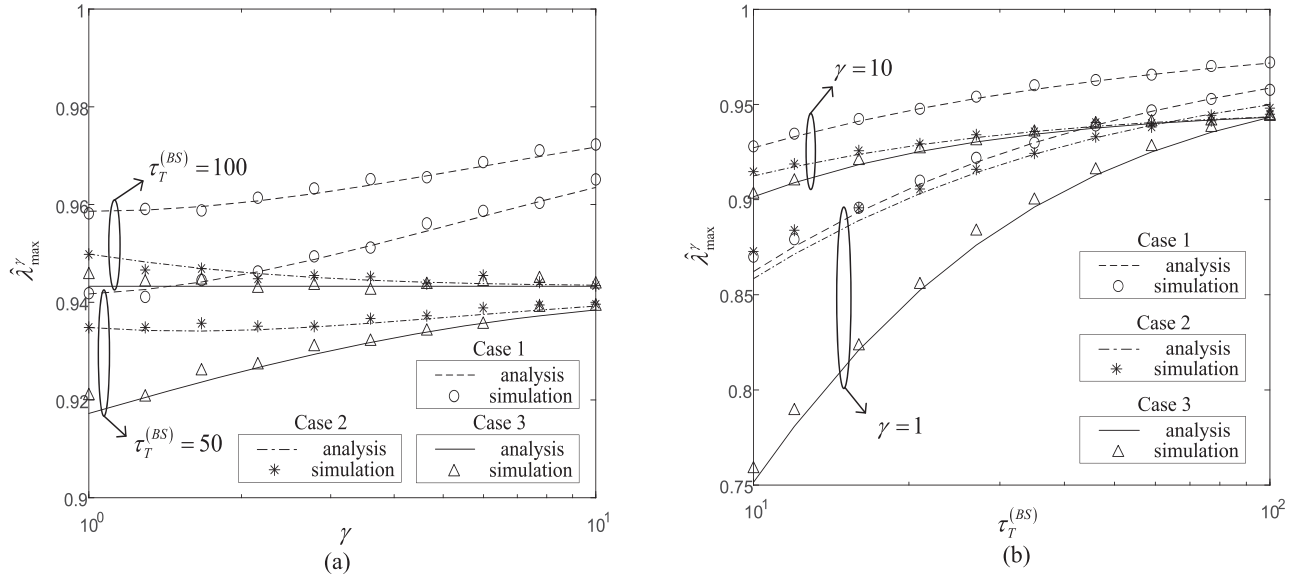


Fig. 6. (a) The maximum total throughput of the coexisting and WiFi networks  $\hat{\lambda}_{\max}^{\gamma}$  versus the throughput ratio between the WiFi and coexisting network  $\gamma$  in three coexistence cases.  $\tau_T^{(BS)}$  is set to be 50 and 100, respectively. (b)  $\hat{\lambda}_{\max}^{\gamma}$  versus the successful transmission time of the coexisting network  $\tau_T^{(BS)}$  (in unit of time slots) in three coexistence cases.  $\gamma$  is set to be 1 and 10, respectively. In both two figures,  $\tau_T^{(W)} = 100$  and  $\tau_F = 10$ .  $W_i^{(W)} = W^{(W)} \cdot \omega(i)$  where  $\omega(i) = \min\{2^i, 2^{K^{(W)}}\}$  and  $K^{(W)} = 6$ .  $W_i^{(BS)} = W^{(BS)} \cdot \zeta(i)$  in which  $\zeta(i) = \min\{2^i, 2^{K^{(BS)}}\}$  and  $K^{(BS)} = 6$ .

the throughputs of both coexisting network and WiFi. Similar observation can be made when  $n^{(W)}$  is fixed. In this case, the increase of  $n^{(BS)}$  from single to multiple would also result in worse throughput performance of both two networks. This is in sharp contrast with the observation from Fig. 5(a) that, in the coexistence system without optimization, a larger number of BSs or WiFi links might improve the throughput of the network where the links belong. This is because the fairness constraint maintains a fixed level of competition between the coexisting and WiFi networks. An increment of the number of links from single to multiple introduces internal competition among the links in this network, leading to the deterioration of throughput performance of its own as well as the whole coexistence system.

It should be noted that, in Case 2 and 3, the maximum total throughputs under fairness constraint do not vary with the number of links in coexistence system, as (27) and (32) indicate. For instance, the competition caused by the variation in multiple links, like  $n^{(BS)}$  or  $n^{(W)}$  changing from 20 to 50, would be balanced by carefully tuning the initial backoff window size of the corresponding network, and thus the optimal performance of both the networks would not be influenced. When the number of links in either network changes from one to more, nevertheless, as Fig. 6(a) and (b) show, intense internal competition emerges in this network and thus its throughput performance deteriorates.

Fig. 6(a) further shows the effect of the target throughput ratio  $\gamma$  on maximum total throughput,  $\hat{\lambda}_{\max}^{\gamma}$ . It can be observed that when  $\gamma$  increases, the gap between the maximum total throughput in Case 2 and that in Case 3,  $\hat{\lambda}_{\max}^{2,\gamma}$  and  $\hat{\lambda}_{\max}^{3,\gamma}$ , is narrowed. This is because as  $\gamma$  increases, the throughput of the WiFi network takes a larger proportion in the total throughput, which marginalizes the effect of the number of BSs. As  $\gamma \rightarrow +\infty$ , the

maximum total throughput in Case 1 can be derived as

$$\lim_{\gamma \rightarrow +\infty} \hat{\lambda}_{\max}^{1,\gamma} = \frac{\tau_T^{(W)}}{1 + \tau_T^{(W)}}, \quad (35)$$

according to (22). For Case 2 and Case 3, we have

$$\lim_{\gamma \rightarrow +\infty} \hat{\lambda}_{\max}^{2,\gamma} = \lim_{\gamma \rightarrow +\infty} \hat{\lambda}_{\max}^{3,\gamma} = \frac{\tau_T^{(W)}}{\tau_T^{(W)} + \tau_F \left( \frac{\tau_T^{(W)}}{-\mathbb{W}_0\left(-\frac{1}{e(1+1/\tau_F)}\right)} - 1 \right)}, \quad (36)$$

according to (27) and (32), respectively. It is indicated in (35) and (36) that as  $\gamma$  increases, the maximum total throughputs in Case 2 and Case 3 tend to be the same, while the maximum total throughput in Case 1 is larger than both of them.

As  $\gamma$  decreases, on the other hand, the gap between the maximum total throughput in Case 1 and that in Case 2,  $\hat{\lambda}_{\max}^{1,\gamma}$  and  $\hat{\lambda}_{\max}^{2,\gamma}$ , is narrowed for a similar reason. As  $\gamma \rightarrow 0$ , we have

$$\lim_{\gamma \rightarrow 0} \hat{\lambda}_{\max}^{1,\gamma} = \lim_{\gamma \rightarrow 0} \hat{\lambda}_{\max}^{2,\gamma} = \frac{\tau_T^{(BS)}}{1 + \tau_T^{(BS)}}, \quad (37)$$

according to (22) and (27). For Case 3 we have

$$\lim_{\gamma \rightarrow 0} \hat{\lambda}_{\max}^{3,\gamma} = \frac{\tau_T^{(BS)}}{\tau_T^{(BS)} + \tau_F \left( \frac{\tau_T^{(BS)}}{-\mathbb{W}_0\left(-\frac{1}{e(1+1/\tau_F)}\right)} - 1 \right)}, \quad (38)$$

according to (32), which is smaller than the limits of maximum total throughputs in Case 1 and Case 2.

The maximum total throughput is not only determined by the target throughput ratio  $\gamma$ , but also the successful transmission

time of coexisting network,  $\tau_T^{(BS)}$ . Contrary to the results in Fig. 5(a) and (b) that a larger  $\tau_T^{(BS)}$  can increase the throughput of coexisting network and reduce WiFi throughput, it can be found in Fig. 6(b) that with a constant  $\gamma$ ,  $\hat{\lambda}_{\max}^{\gamma}$  is improved as  $\tau_T^{(BS)}$  increases, indicating that both the throughput performances of the coexisting and WiFi networks are enhanced. In addition, it is indicated in Fig. 6(b) that when  $\tau_T^{(BS)}$  increases, the gap between  $\hat{\lambda}_{\max}^{2,\gamma}$  and  $\hat{\lambda}_{\max}^{3,\gamma}$  is narrowed. The reason is that when both the initial backoff window sizes of BSs and WiFi links in Case 2 and Case 3,  $W^{(BS)}$  and  $W^{(W)}$ , are jointly tuned according to (30), (31) and (33), (34), respectively,  $W^{(W)}$  decreases as  $\tau_T^{(BS)}$  increases. Therefore, the contention from the WiFi network becomes fiercer for the coexisting network, which marginalizes the influence of  $n^{(BS)}$ . As  $\tau_T^{(BS)} \rightarrow +\infty$ , we have

$$\lim_{\tau_T^{(BS)} \rightarrow +\infty} \hat{\lambda}_{\max}^{1,\gamma} = \frac{\tau_T^{(W)}}{1+\gamma} + \tau_T^{(W)}, \quad (39)$$

$$\lim_{\tau_T^{(BS)} \rightarrow +\infty} \hat{\lambda}_{\max}^{2,\gamma} = \frac{\frac{1+\gamma}{\gamma} \cdot \tau_T^{(W)}}{\tau_T^{(W)} + \tau_F \left( \frac{1}{-\mathbb{W}_0\left(-\frac{1}{e(1+1/\tau_F)}\right)} - 1 \right)}, \quad (40)$$

$$\lim_{\tau_T^{(BS)} \rightarrow +\infty} \hat{\lambda}_{\max}^{3,\gamma} = \frac{\frac{1+\gamma}{\gamma} \cdot \tau_T^{(W)}}{\left(1 + \frac{1}{\gamma}\right) \tau_T^{(W)} + \tau_F \left( \frac{1}{-\mathbb{W}_0\left(-\frac{1}{e(1+1/\tau_F)}\right)} - 1 \right)}, \quad (41)$$

according to (22), (27), and (32), respectively. The comparison among (39), (40), and (41) shows that with a large  $\gamma$ , the maximum total throughput in Case 1 is larger than that in Case 2 and Case 3, and  $\hat{\lambda}_{\max}^{2,\gamma}$  and  $\hat{\lambda}_{\max}^{3,\gamma}$  are getting close to each other while  $\hat{\lambda}_{\max}^{2,\gamma}$  is slightly larger as  $\tau_T^{(BS)} \rightarrow +\infty$ .

With a smaller  $\tau_T^{(BS)}$ , on the other hand, it is illustrated in Fig. 6(b) that as  $\tau_T^{(BS)}$  decreases, the gap between  $\hat{\lambda}_{\max}^{1,\gamma}$  and  $\hat{\lambda}_{\max}^{2,\gamma}$  becomes smaller. This is because when both the initial backoff window sizes of the coexisting and WiFi networks in Case 1 and Case 2,  $W^{(BS)}$  and  $W^{(W)}$ , are jointly tuned according to (25), (26) and (30), (31), respectively, the decrease of  $\tau_T^{(BS)}$  leads to the decrease of  $W^{(BS)}$ , with which the BS gains competitive advantage against the WiFi network. As a result, the BS gradually takes a predominant place, alleviating the influence of  $n^{(W)}$  over the coexistence system.

## V. CONCLUSION

In this paper, we study the impact of the number of links on LAA-WiFi coexistence in unlicensed bands. The throughput performances of the coexisting network and WiFi under all the three cases are characterized as explicit expressions. By comparing the network throughputs in different cases, it is shown that given successful transmission time and collision time, how the change in the number of links would affect network performance largely depends on the initial backoff window size.

The maximum total throughput of the coexisting network and WiFi under the throughput fairness and the corresponding

initial backoff window sizes are further characterized as explicit expressions, indicating that a fair and efficient coexistence can be achieved by jointly adjusting the initial backoff window sizes of both two networks. A comparison among the optimal throughput performance of three cases is conducted, where it is shown that the variation of the number of multiple links in one case would not affect optimal total throughput, since the initial backoff window sizes are carefully tuned to balance the competition. The drastic change from single link to multiple links in one network, nevertheless, can yield fierce internal competition in this network, and thus deteriorates both the optimal throughputs of the coexisting network and WiFi. As a result, Case 1 has the best maximum total throughput among all the three cases, indicating that the inclusion of uplink transmissions for LAA in 3GPP R14 might lead to performance deterioration compared with R13, which considers only the downlink transmissions of LAA. This work sheds important light on the protocol design of LAA-WiFi coexistence. In the future, the study can be further extended to the spectrum sharing between 5G NR-U and WiFi.

## APPENDIX A PROOF OF THEOREM 1

*Proof:* Given  $\frac{\hat{\lambda}_{\text{out}}^{(W)}}{\hat{\lambda}_{\text{out}}^{(BS)}} = \gamma > 0$ , we have

$$p^{(W)} = \frac{\gamma \tau_T^{(BS)} p^{(BS)}}{\tau_T^{(W)} (1 - p^{(BS)}) + \gamma \tau_T^{(BS)} p^{(BS)}}. \quad (42)$$

Let  $\hat{\lambda}_{\text{out}} = \hat{\lambda}_{\text{out}}^{(W)} + \hat{\lambda}_{\text{out}}^{(BS)}$ . By combining  $\frac{\hat{\lambda}_{\text{out}}^{(W)}}{\hat{\lambda}_{\text{out}}^{(BS)}} = \gamma$ , (14) and (42), we have

$$\hat{\lambda}_{\text{out}} = \frac{1+\gamma}{\gamma} \cdot \frac{\tau_T^{(W)}}{\frac{\tau_T^{(W)} + \tau_F \tau_T^{(W)} (1-p^{(BS)})}{\gamma \tau_T^{(BS)} p^{(BS)}} + \frac{1}{1-p^{(BS)}} + \frac{1+\gamma}{\gamma} \cdot \tau_T^{(W)}}. \quad (43)$$

Let  $h(p^{(BS)}) = \frac{\tau_T^{(W)} + \tau_F \tau_T^{(W)} (1-p^{(BS)})}{\gamma \tau_T^{(BS)} p^{(BS)}} + \frac{1}{1-p^{(BS)}}$ . Maximizing  $\hat{\lambda}_{\text{out}}$  is therefore converted to minimize  $h(p^{(BS)})$ . It is obtained that  $\frac{dh(p^{(BS)})}{dp^{(BS)}} < 0$  if  $p^{(BS)} < p^{\gamma, (BS)}$ , and  $\frac{dh(p^{(BS)})}{dp^{(BS)}} > 0$  if  $p^{(BS)} > p^{\gamma, (BS)}$ , where  $p^{\gamma, (BS)}$  is the single root of  $\frac{dh(p^{(BS)})}{dp^{(BS)}} = 0$ , and is given by (23). As a result,  $h(p^{(BS)})$  is minimized at  $p^{(BS)} = p^{\gamma, (BS)}$ . (22) can then be obtained by substituting  $p^{(BS)} = p^{\gamma, (BS)}$  into (43). ■

## APPENDIX B PROOF OF THEOREM 2

*Proof:* According to (19) we have

$$\alpha_A = -\frac{1}{p_A \ln p_A} \sum_{g=BS,W} \frac{\hat{\lambda}_{\text{out}}^{3,(g)}}{\tau_T^{(g)}}. \quad (44)$$

And it can be obtained that

$$1 + \tau_F - \tau_F p_A - \left( \frac{\sum_{g=BS,W} \tau_T^{(g)} X^{(g)}}{\sum_{g=BS,W} X^{(g)}} - \tau_F \right) p_A \ln p_A = \frac{1}{\alpha_A}, \quad (45)$$

according to (20). Substituting (44) into (45) results in

$$-p_A \ln p_A = \left[ 1 + \tau_F - \tau_F p_A - \left( \frac{\sum_{g=BS,W} \tau_T^{(g)} X^{(g)}}{\sum_{g=BS,W} X^{(g)}} - \tau_F \right) \cdot p_A \ln p_A \right] \sum_{g=BS,W} \frac{\hat{\lambda}_{out}^{3,(g)}}{\tau_T^{(g)}}, \quad (46)$$

which can be reduced to

$$\hat{\lambda}_{out}^{3,(BS)} = \frac{1}{1 + \gamma + \frac{\gamma \tau_T^{(BS)} + \tau_T^{(W)}}{\tau_T^{(BS)} \tau_T^{(W)}} \cdot \left( \frac{1 + \tau_F - \tau_F p_A}{-p_A \ln p_A} - \tau_F \right)}. \quad (47)$$

Therefore, the restrained optimization problem in (21) can be rewritten as

$$\begin{aligned} & \max_{\{W^{(BS)}, W^{(W)}\}} (\hat{\lambda}_{out}^{3,(BS)} + \hat{\lambda}_{out}^{3,(W)}) \\ &= \max_{\{W^{(BS)}, W^{(W)}\}} (1 + \gamma) \hat{\lambda}_{out}^{3,(BS)} \\ &= \max_{\{W^{(BS)}, W^{(W)}\}} \frac{1 + \gamma}{1 + \gamma + \frac{\gamma \tau_T^{(BS)} + \tau_T^{(W)}}{\tau_T^{(BS)} \tau_T^{(W)}} \cdot \left( \frac{1 + \tau_F - \tau_F p_A}{-p_A \ln p_A} - \tau_F \right)}, \end{aligned} \quad (48)$$

which is equal to

$$\min_{\{W^{(BS)}, W^{(W)}\}} \frac{1 + \tau_F - \tau_F p_A}{-p_A \ln p_A}. \quad (49)$$

Let us denote  $f(p_A) = \frac{1 + \tau_F - \tau_F p_A}{-p_A \ln p_A}$ . The derivative of  $f(p_A)$  is given by

$$\frac{df(p_A)}{dp_A} = \frac{(1 + \tau_F)(1 + \ln p_A) - \tau_F p_A}{(-p_A \ln p_A)^2}. \quad (50)$$

Denote  $g(p_A) = (1 + \tau_F)(1 + \ln p_A) - \tau_F p_A$ , and we have

$$p_A^* = -(1 + 1/\tau_F) \mathbb{W}_0 \left( -\frac{1}{e(1 + 1/\tau_F)} \right), \quad (51)$$

which is the root of  $g(p_A) = 0$ .  $g(p_A) < 0$  if  $p_A \in (0, p_A^*)$ , and  $g(p_A) > 0$  if  $p_A \in (p_A^*, 1)$ . Therefore, it can be concluded that  $f(p_A)$  is monotonically decreasing with  $p_A$  if  $p_A \in (0, p_A^*)$ , and is increasing with  $p_A$  if  $p_A \in (p_A^*, 1)$ . So the minimum value is achieved at  $p_A = p_A^*$ . The solution to (48) can then be given by

$$\begin{aligned} & \max(\hat{\lambda}_{out}^{3,(BS)} + \hat{\lambda}_{out}^{3,(W)}) \\ &= \frac{1 + \gamma}{1 + \gamma + \frac{\gamma \tau_T^{(BS)} + \tau_T^{(W)}}{\tau_T^{(BS)} \tau_T^{(W)}} \cdot \left( \frac{1 + \tau_F - \tau_F p_A^*}{-p_A^* \ln p_A^*} - \tau_F \right)}. \end{aligned} \quad (52)$$

According to (19), when the total throughput is optimized, it should satisfy that

$$-\ln p_A^* = \sum_{g=BS,W} \frac{2n^{(g)}}{\sum_{i=0}^{\infty} p_A^* (1 - p_A^*)^i \cdot W_i^{(g)} + (1 - p_A^*)^{K^{(g)}} \cdot W_{K^{(g)}}^{(g)}}. \quad (53)$$

Combine  $\frac{\hat{\lambda}_{out}^{3,(W)}}{\hat{\lambda}_{out}^{3,(BS)}} = \gamma$  with (18), and we have

$$\begin{aligned} & \frac{\gamma n^{(BS)} \tau_T^{(BS)}}{W^{(BS)} \cdot \left( \sum_{i=0}^{\infty} p_A^* (1 - p_A^*)^i \zeta(i) + (2 - 2p_A^*)^{K^{(BS)}} \right)} \\ &= \frac{n^{(W)} \tau_T^{(W)}}{W^{(W)} \cdot \left( \sum_{i=0}^{\infty} p_A^* (1 - p_A^*)^i \omega(i) + (2 - 2p_A^*)^{K^{(W)}} \right)}. \end{aligned} \quad (54)$$

The corresponding optimal initial backoff window sizes, (33) and (34), can then be derived by substituting (54) into (53). ■

## REFERENCES

- [1] J. Li, X. Wang, D. Feng, M. Sheng, and T. Q. S. Quek, "Share in the commons: Coexistence between LTE unlicensed and Wi-Fi," *IEEE Wireless Commun.*, vol. 23, no. 6, pp. 16–23, Dec. 2016.
- [2] C. Cano, D. López-Pérez, H. Claussen, and D. Leith, "Using LTE in unlicensed bands: Potential benefits and coexistence issues," *IEEE Commun. Mag.*, vol. 54, no. 12, pp. 116–123, Dec. 2016.
- [3] C. Cano and D. J. Leith, "Unlicensed LTE/WiFi coexistence: Is LBT inherently fairer than CSAT?," in *Proc. IEEE Int. Conf. Commun.*, 2016, pp. 1–6.
- [4] A. D. Shoaei, M. Derakhshani, and T. Le-Ngoc, "Efficient LTE/Wi-Fi coexistence in unlicensed spectrum using virtual network entity: Optimization and performance analysis," *IEEE Trans. Commun.*, vol. 66, no. 6, pp. 2617–2629, Jun. 2018.
- [5] Y. Jian, C.-F. Shih, B. Krishnaswamy, and R. Sivakumar, "Coexistence of Wi-Fi and LAA-LTE: Experimental evaluation, analysis and insights," in *Proc. IEEE Int. Conf. Commun. Workshop*, 2015, pp. 2325–2331.
- [6] F. M. Abinader et al., "Enabling the coexistence of LTE and Wi-Fi in unlicensed bands," *IEEE Commun. Mag.*, vol. 52, no. 11, pp. 54–61, Nov. 2014.
- [7] N. Jindal and D. Breslin, "LTE and Wi-Fi in unlicensed spectrum: A coexistence study," Google, Washington, D.C., USA, White Paper, 2015.
- [8] A. M. Cavalcante et al., "Performance evaluation of LTE and Wi-Fi coexistence in unlicensed bands," in *Proc. IEEE 77th Veh. Technol. Conf.*, 2013, pp. 1–6.
- [9] *Technical specification group radio access network; study on licensed-assisted access to unlicensed spectrum; release 13*, document 3GPP-36889-d00, 3GPP, 2015.
- [10] H.-J. Kwon et al., "Licensed-assisted access to unlicensed spectrum in LTE release 13," *IEEE Commun. Mag.*, vol. 55, no. 2, pp. 201–207, Feb. 2017.
- [11] R. Ratasuk, N. Mangalvedhe, and A. Ghosh, "LTE in unlicensed spectrum using licensed-assisted access," in *Proc. IEEE Globecom Workshops*, 2014, pp. 746–751.
- [12] FCC, "Report and order and further notice of proposed rule-making; in the matter of unlicensed use of the 6 GHz band (et docket no 18-295); expanding flexible use in mid-band spectrum between 3.7 and 24 GHz (GN docket no. 17-183)," 2020. [Online]. Available: <https://docs.fcc.gov/public/attachments/FCC-20-51A1.pdf>
- [13] G. Naik and J.-M. J. Park, "Coexistence of Wi-Fi 6E and 5 G NR-U: Can we do better in the 6 GHz bands?," in *Proc. IEEE Conf. Comput. Commun.*, 2021, pp. 1–10.
- [14] *Technical specification group radio access network; study on nr-based access to unlicensed spectrum release 16*, 3GPP, 2018.
- [15] R. Saleem, S. A. Alvi, and S. Durrani, "Performance-fairness trade-off for Wi-Fi and LTE-LAA coexistence," *IEEE Access*, vol. 9, pp. 62446–62459, 2021.
- [16] G. Naik, J.-M. Park, J. Ashdown, and W. Lehr, "Next generation Wi-Fi and 5 G NR-U in the 6 GHz bands: Opportunities and challenges," *IEEE Access*, vol. 8, pp. 153027–153056, 2020.
- [17] A. K. Bairagi et al., "Coexistence mechanism between eMBB and uRLLC in 5 G wireless networks," *IEEE Trans. Commun.*, vol. 69, no. 3, pp. 1736–1749, Mar. 2021.
- [18] M. Alsenwi, N. H. Tran, M. Bennis, S. R. Pandey, A. K. Bairagi, and C. S. Hong, "Intelligent resource slicing for eMBB and URLLC coexistence in 5 G and beyond: A deep reinforcement learning based approach," *IEEE Trans. Wireless Commun.*, vol. 20, no. 7, pp. 4585–4600, Jul. 2021.



- [19] M. Alsenwi, N. H. Tran, M. Bennis, A. K. Bairagi, and C. S. Hong, "eMBS-URLLC resource slicing: A risk-sensitive approach," *IEEE Commun. Lett.*, vol. 23, no. 4, pp. 740–743, Apr. 2019.
- [20] F. Luo, X. Sun, Y. Gao, W. Zhao, P. Liu, and Z. Guo, "Optimal coexistence of NR-U with Wi-Fi under 3GPP fairness constraint," in *IEEE Int. Conf. Commun.*, pp. 4890–4895, 2022.
- [21] T. Tao, F. Han, and Y. Liu, "Enhanced LBT algorithm for LTE-LAA in unlicensed band," in *Proc. IEEE 26th Annu. Int. Symp. Pers. Indoor Mobile Radio Commun.*, 2015, pp. 1907–1911.
- [22] G. J. Sutton, R. P. Liu, and Y. J. Guo, "Delay and reliability of load-based listen-before-talk in LAA," *IEEE Access*, vol. 6, pp. 6171–6182, 2018.
- [23] Y. Song, K. W. Sung, and Y. Han, "Coexistence of Wi-Fi and cellular with listen-before-talk in unlicensed spectrum," *IEEE Commun. Lett.*, vol. 20, no. 1, pp. 161–164, Jan. 2016.
- [24] C. Cano, D. J. Leith, A. Garcia-Saavedra, and P. Serrano, "Fair coexistence of scheduled and random access wireless networks: Unlicensed LTE/WiFi," *IEEE/ACM Trans. Netw.*, vol. 25, no. 6, pp. 3267–3281, Dec. 2017.
- [25] *Part 11: Wireless LAN Medium Access Control (MAC) and Physical Layer (PHY) Specifications*, IEEE Standard 802.11-2012, 2012.
- [26] V. Valls, A. Garcia-Saavedra, X. Costa, and D. J. Leith, "Maximizing LTE capacity in unlicensed bands (LTE-U/LAA) while fairly coexisting with 802.11 WLANs," *IEEE Commun. Lett.*, vol. 20, no. 6, pp. 1219–1222, Jun. 2016.
- [27] Y. Ma and D. G. Kuester, "MAC-Layer coexistence analysis of LTE and WLAN systems via listen-before-talk," in *Proc. IEEE 14th Annu. Consum. Commun. Netw. Conf.*, 2017, pp. 534–541.
- [28] Y. Li, T. Zhou, Y. Yang, H. Hu, and M. Hamalainen, "Fair downlink traffic management for hybrid LAA-LTE/Wi-Fi networks," *IEEE Access*, vol. 5, pp. 7031–7041, 2017.
- [29] J. Zhang, S. Liu, R. Yin, G. Yu, and X. Jin, "Coexistence algorithms for LTE and WiFi networks in unlicensed spectrum: Performance optimization and comparison," *Wireless Netw.*, vol. 27, no. 3, pp. 1875–1885, 2021.
- [30] M. Mehrnosh, V. Sathya, S. Roy, and M. Ghosh, "Analytical modeling of Wi-Fi and LTE-LAA coexistence: Throughput and impact of energy detection threshold," *IEEE/ACM Trans. Netw.*, vol. 26, no. 4, pp. 1990–2003, Aug. 2018.
- [31] R. Yin, G. Yu, A. Maaref, and G. Y. Li, "LBT-Based adaptive channel access for LTE-U systems," *IEEE Trans. Wireless Commun.*, vol. 15, no. 10, pp. 6585–6597, Oct. 2016.
- [32] E. Baena, S. Fortes, and R. Barco, "KQI performance evaluation of 3GPP LBT priorities for indoor unlicensed coexistence scenarios," *Electronics*, vol. 9, no. 10, 2020, Art. no. 1701.
- [33] M. Alhulayil and M. Lopez-Benitez, "Novel LAA waiting and transmission time configuration methods for improved LTE-LAA/Wi-Fi coexistence over unlicensed bands," *IEEE Access*, vol. 8, pp. 162373–162393, 2020.
- [34] B. Bojovic, L. Giupponi, Z. Ali, and M. Miozzo, "Evaluating unlicensed LTE technologies: LAA vs LTE-U," *IEEE Access*, vol. 7, pp. 89714–89751, 2019.
- [35] Qualcomm, "LTE in unlicensed spectrum: Harmonious coexistence with Wi-Fi," Qualcomm Research, Qualcomm, 2014.
- [36] S. Saadat, W. Ejaz, S. Hassan, I. Bari, and T. Hussain, "Enhanced network sensitive access control scheme for LTE-LAA/Wi-Fi coexistence: Modeling and performance analysis," *Comput. Commun.*, vol. 172, pp. 45–53, 2021.
- [37] A. M. Baswade et al., "Performance analysis of spatially distributed LTE-U/NR-U and Wi-Fi networks: An analytical model for coexistence study," *J. Netw. Comput. Appl.*, vol. 191, 2021, Art. no. 103157.
- [38] J. Zheng, J. Xiao, Q. Ren, and Y. Zhang, "Performance modeling of an LTE LAA and WiFi coexistence system using the LAA Category-4 LBT procedure and 802.11e EDCA mechanism," *IEEE Trans. Veh. Technol.*, vol. 69, no. 6, pp. 6603–6618, Jun. 2020.
- [39] X. Sun and L. Dai, "Towards fair and efficient spectrum sharing between LTE and WiFi in unlicensed bands: Fairness-constrained throughput maximization," *IEEE Trans. Wireless Commun.*, vol. 19, no. 4, pp. 2713–2727, Apr. 2020.
- [40] X. Sun, J. Zhang, V. C. Leung, and H. Zhu, "Achieving optimum throughput for LTE and WiFi coexistence," in *Proc. IEEE Wireless Commun. Signal Process.*, pp. 1–6, 2017.
- [41] L. Dai and X. Sun, "A unified analysis of IEEE 802.11 DCF networks: Stability, throughput, and delay," *IEEE Trans. Mobile Comput.*, vol. 12, no. 8, pp. 1558–1572, Aug. 2013.
- [42] Y. Gao, "LTE-LAA and WiFi in 5G NR unlicensed: Fairness, optimization and win-win solution," *IEEE SmartWorld, Ubiquitous Intell. Comput., Adv. Trusted Comput., Scalable Comput. Commun. Cloud Big Data Comput. Internet People Smart City Innov.*, 2019, pp. 1638–1643.



**Yingqi Lin** received the B.Eng. degree in electronic information science and technology from Sun Yat-sen University, Guangzhou, China, in 2021. She is currently working toward the M.S. degree in electrical engineering and information technology with ETH Zurich, Zurich, Switzerland. Her research interests include signal processing, Internet of Things, and machine learning for wireless communication systems.



**Xinghua Sun** (Member, IEEE) received the B.S. degree from the Nanjing University of Posts and Telecommunications (NJUPT), Nanjing, China, in 2008, and the Ph.D. degree from the City University of Hong Kong (CityU), Hong Kong, in 2013. In 2010, he was a visiting student with the National Institute for Research in Digital Science and Technology (INRIA), France. In 2013, he was a Postdoctoral Fellow with CityU. From 2014 to 2018, he was an Associate Professor with NJUPT. From 2015 to 2016, he was a Postdoctoral Fellow with University of British Columbia, Vancouver, BC, Canada. Since 2018, he has been an Associate Professor with Sun Yat-sen University, Guangzhou, China. From July to August 2019, he was a Visiting Scholar with the Singapore University of Technology and Design, Singapore. His research interests include stochastic modeling of wireless networks and machine learning for networking. Dr. Sun was the Technical Program Committee Member for numerous IEEE conferences.



**Yayu Gao** (Member, IEEE) received the B.S. degree in electronic engineering from the Nanjing University of Posts and Telecommunications, Nanjing, China, in 2009, and the Ph.D. degree in electronic engineering from the City University of Hong Kong, Kowloon, Hong Kong, in 2014. Since March 2014, she has been with the School of Electronic Information and Communication, Huazhong University of Science and Technology, Wuhan, China, where she is an Associate Professor. Her research interests include random access networks, next-generation WiFi networks, heterogeneous network coexistence, and network intelligence.



**Wen Zhan** (Member, IEEE) received the B.S. and M.S. degrees from the University of Electronic Science and Technology of China, Chengdu, China, in 2012 and 2015, respectively, and the Ph.D. degree from the City University of Hong Kong, China, in 2019. He was a Research Assistant and a Postdoctoral Fellow with the City University of Hong Kong. Since 2020, He has been with the School of Electronics and Communication Engineering, Sun Yat-sen University, Guangzhou, China, where he is currently an Assistant Professor. His research interests include Internet of Things, modeling, and performance optimization of next-generation mobile communication systems.





China. His research interests include age of information, Internet of Things, and UAV communications.

**Xijun Wang** (Member, IEEE) received the B.S. degree in communications engineering from Xidian University Xi'an, China, in 2005, and the Ph.D. degree in electronic engineering from Tsinghua University, Beijing, China, in January 2012. He was an Assistant Professor from 2012 to 2015 and an Associate Professor with Xidian University, from 2015 to 2018. From 2015 to 2016, he was a Research Fellow with the Singapore University of Technology and Design, Singapore. He is currently an Associate Professor with Sun Yat-sen University, Guangzhou,



In July 2005 and from September 2006 to April 2007, he visited NTT DoCoMo Research and Development (YRP), Japan, and Wireless Communications and Signal Processing (WCSP) Lab, National Tsing Hua University, Hsinchu, Taiwan. His research interests mainly include 5G wireless and mobile communication networks, the Internet of Things (IoT).

**Xiang Chen** (Member, IEEE) received the B.E. and Ph.D. degrees from the Department of Electronic Engineering, Tsinghua University, Beijing, China, in 2002 and 2008, respectively. From July 2008 to December 2014, he was with the Wireless and Mobile 1020 Communication Technology Research and Development Center (Wireless Center), and Aerospace 1022 Center, Tsinghua University, respectively. Since January 2015, he has been an Associate Professor with the School of Electronics and Information Technology, Sun Yat-sen University, Guangzhou, China.